Liquid-Crystalline Collapse of Pulmonary Surfactant Monolayers

William R. Schief,* Meher Antia,† Bohdana M. Discher,‡ Stephen B. Hall,‡§‖ and Viola Vogel†*

Departments of †Bioengineering and *Physics, University of Washington, Seattle, Washington 98195; and ‡Departments of Biochemistry and Molecular Biology, §Medicine, and ‖Physiology and Pharmacology, Oregon Health & Science University, Portland, Oregon 97239

ABSTRACT During exhalation, the surfactant film of lipids and proteins that coats the alveoli in the lung is compressed to high surface pressures, and can remain metastable for prolonged periods at pressures approaching 70 mN/m. Monolayers of calf lung surfactant extract (CLSE), however, collapse in vitro, during an initial compression at ~45 mN/m. To gain information on the source of this discrepancy, we investigated how monolayers of CLSE collapse from the interface. Observations with fluorescence, Brewster angle, and light scattering microscopies show that monolayers containing CLSE, CLSE-cholesterol (20%), or binary mixtures of dipalmitoyl phosphatidylcholine(DPPC)-dihydrocholesterol all form bilayer disks that reside above the monolayer. Upon compression and expansion, lipids flow continuously from the monolayer into the disks, and vice versa. In several respects, the mode of collapse resembles the behavior of other amphiphiles that form smectic liquid-crystal phases. These findings suggest that components of surfactent films must collapse collectively rather than being squeezed out individually.

INTRODUCTION

In the lung, a thin layer of liquid lines the alveolar air‖ spaces (Bastacky et al., 1995), and the surface tension of the resulting air-liquid interface provides an inward pull that tends to cause deflation. A complex mixture of lipids and proteins, synthesized and secreted into the liquid layer by the type II pneumocytes, acts as a surfactant, adsorbing to the interface and reducing surface tension. When compressed by the decreasing alveolar surface area during exhalation, surfactant films in situ reach and sustain for prolonged periods surface pressures approaching 70 mN/m (Horie and Hildebrandt, 1971; Schürch, 1982), thereby minimizing surface tension and stabilizing the alveoli, particularly at small volumes.

This behavior of the surfactant films in situ is exceptional. Interfacial monolayers exist under equilibrium conditions only up to a maximum surface pressure at which they undergo a two-to-three dimensional phase transition commonly known as collapse. Surface films can persist in metastable forms at higher surface pressures, but only if they are sufficiently rigid to resist flow into the third dimension. The quasi-static surface pressure-area isotherm (π-A) for monolayers of pulmonary surfactant, like other films that contain a preponderance of fluid phospholipids, has a broad plateau at a pressure of ~45 mN/m that indicates collapse and that prevents access to higher surface pressures (Crane and Hall, 2001). The markedly different behavior in vitro and in situ indicates that in the lungs, the films undergo some transformation to metastable structures that can avoid collapse (Piknova et al., 2002).

A better understanding of the mechanism by which lung surfactant is transformed in vivo may be gained from the details of collapse. Studies of lipid or lipid-protein monolayers at the air-water interface in Langmuir troughs have revealed a variety of processes. In highly compressed monolayers, the modes of collapse include the following: linear folding for cholesterol, cerebronic acid, and 2-hydroxytetracosanoic acid (Ries, 1979; Ries and Swift, 1987; Ybert et al., 2002); buckling for charged copolymers (Fontaine et al., 1997), and for distearoyl phosphatidylcholine (Saint-Jalmes et al., 1994; Saint-Jalmes and Gallet, 1998); three-dimensional crystal formation for mixtures of cholesterol and dipalmitoyl phosphatidylcholine (DPPC) (Worthman et al., 1997; Lafont et al., 1998); and nanoscale budding for plain DPPC (Schief et al., 2000a). All of these modes, with the exception of 2-hydroxytetracosanoic acid, involve collapse toward the air. Model films of lung surfactant that contain some of its phospholipids and proteins collapse by still different mechanisms. For example, mixtures of dipalmitoyl phosphatidylglycerol and palmitoyl-oleoyl phosphatidylglycerol with and without the lung surfactant proteins SP-B and SP-C, which form coexisting fluid and condensed monolayer phases, buckle into extended folds toward the water (Lipp et al., 1998; Gopal and Lee, 2001; Takamoto et al., 2001). Mixtures of DPPC, dipalmitoyl phosphatidylglycerol, and SP-C, also in a fluid/condensed phase coexistence, collapse via multilamellar layering at the edges of condensed monolayer domains (Amrein et al., 1997; Kramer et al., 2000).

The diversity of mechanisms by which different monolayers collapse raises the crucial question of which process is

Submitted October 31, 2002, and accepted for publication January 28, 2003.

Address reprint requests to Stephen B. Hall, Molecular Medicine, Mail Code NRC-3, OHSU, Portland, OR 97239. Tel.: 503-494-6667; Fax: 503-494-7368; E-mail: sbh@ohsu.edu or Viola Vogel, Dept. of Bioengineering, Box 351721, University of Washington, Seattle, WA 98195. Tel.: 206-543-1776; Fax: 206-685-4434; E-mail: vvogel@u.washington.edu.

William R. Schief's present address is Dept. of Biochemistry, University of Washington, Seattle, WA 98195.

Bohdana M. Discher's present address is Dept. of Biochemistry and Biophysics, University of Pennsylvania, 422 Curie Blvd., Philadelphia, PA 19104-6059.

0006-3495/03/06/3792/15 $2.00

most relevant to the function of pulmonary surfactant. The complex composition of the biological material makes it difficult to extrapolate from simpler monolayers to the native films. Although a previous study has examined the collapse of porcine surfactant monolayers (Nag et al., 1998), the experiments were unable to provide details about the morphology of the structures formed, nor could they elucidate the mechanism of their formation. We have therefore first carried out a systematic study of collapse in monolayers containing the complete mixture of hydrophobic constituents from calf surfactant. We used Brewster angle microscopy (BAM), light scattering microscopy (LSM), and fluorescence microscopy (FM) to investigate the mechanism by which monolayers of calf lung surfactant extract (CLSE) collapse from the air-water interface. To corroborate our findings and to control for the effects of possible impurities in the biological sample, we then also examined synthetic mixtures of the major surfactant component, DPPC, and an analog of cholesterol, dihydrocholesterol (dchol). We document the similarity of structures formed from the native and model mixtures, the nucleation and growth of the collapsed three-dimensional phase during compression, and its dissolution during expansion. We also characterize the structure, size, and position of the collapsed structures with respect to the monolayer, and provide information on their motion and interactions.

MATERIALS AND METHODS

Materials

CLSE, prepared by previously published protocols (Notter et al., 1983), was provided by Dr. Edmund Egan of ONY (Amherst, NY). DPPC (1,2-dipalmitoyl-*sn*-glycero-3-phosphocholine) and the fluorescent probe 1,2-dipalmitoyl-*sn*-phosphoethanolamine-*N*-[lissamine rhodamine B sulfonyl] (Rh-DPPE) were purchased from Avanti Polar Lipids (Alabaster, AL). Cholesterol and dchol (3β-hydroxy-5α-cholestane) were purchased from Sigma Chemicals (St. Louis, MO). The lipids were dissolved in chloroform:methanol (3:1 v/v) or in pure chloroform and mixed in the desired molar proportions for a final concentration of $\sim$1 mM. Organic solvents were HPLC grade, purchased from Aldrich (Milwaukee, WI).

The fluorescence quenching experiments used a subphase of nanopure water. For all other experiments, the subphase was a buffer at pH 7.0 containing 10 mM Hepes, 150 mM NaCl, and 1.5 mM $CaCl_2$ (HSC). All buffer salts were of highest purity (SigmaUltra, Sigma Chemicals). For the quenching experiments, the stock solutions of $CoCl_2$ (SigmaUltra) had concentrations of 1.7–2 M and pH 7.0. All experiments used water (resistivity >18.0 MΩ, pH 5.6) from a Barnstead (Dubuque, IA) nanopure filtration system.

Methods

Compression isotherms

π-A isotherms of lipid monolayers were measured in a custom-built Teflon trough (maximum area of 532 cm^2) with a continuous perimeter vertical Teflon ribbon from Labcon (Darlington, UK) to contain the film. Solutions were spread to an initial surface pressure no greater than 0.3 mN/m. Before compression, 10 min were allowed for solvent evaporation. Films were compressed and expanded at rates of 1–2 $Å^2$/(molecule $\times$ minute). The temperature of the subphase was maintained at 20°C by pumping water through the base of the trough. Active electronic vibration isolation tables (MOD 2, Nanofilm Technologie, Göttingen, Germany) supported the trough, as well as the microscopes described below.

Brewster angle microscopy

A home-built Brewster angle microscope (Schief et al., 2000a) was used to examine monolayers that contained no added fluorescent probes unless otherwise noted. Brewster angle microscopy (BAM) derives contrast within a film from differences in reflectivity to *p*-polarized light incident at Brewster's angle for the clean air-water interface (Hénon and Meunier, 1991; Hönig and Möbius, 1991; Meunier, 2000).

We have previously analyzed BAM grayscales from lipid monolayers to provide quantitative information on the relative optical thicknesses of different monolayer phases, and the changes in optical thickness with surface pressure (Discher et al., 1999b; Piknova et al., 2001). In the studies reported here, the disks formed by the collapse of CLSE and DPPC/dchol were so highly reflective that they saturated the camera if the analyzer was set to *p*-polarization. We therefore developed a method to extend the dynamic range of the BAM grayscale in a quantitative manner. The extended grayscale extrapolated values measured at a series of analyzer orientations to obtain the grayscale at *p*-polarization. In general, the BAM grayscale of an optically isotropic object will vary with the analyzer angle α according to

$$g(\alpha) = g_0 + g_p \cos^2(\alpha - \alpha_p), \quad (1)$$

where α_p is the absolute position of *p*-polarization on the analyzer rotation stage, g_0 is the fixed arbitrary black level (set manually on the camera control unit), and g_p is the component of the grayscale that is proportional to the reflectivity at *p*-polarization. We refer to g_p as the ''extended'' BAM grayscale at *p*-polarization, because $g_p = g(\alpha_p) - g_0$. When fit to Eq. 1, measurements of $g(\alpha)$ for the monolayer provided values of g_0 and α_p. These constants were then used in Eq. 1 to fit measurements for disks and double disks and to obtain values of g_p for those structures.

Fluorescence microscopy

We examined films that contained 0.3 mol % of the fluorescent probe Rh-DPPE with fluorescence microscopy (FM). Contrast is derived from the probe's different solubility in different regions of the film. The large rhodamine chromophore attached to the headgroup of the Rh-DPPE lowers the solubility of the probe in condensed phases (Von Tscharner and McConnell, 1981; Lösche et al., 1983; Peters and Beck, 1983). A Nikon epifluorescence microscope with an extra-long working distance objective (40$\times$, 9-mm working distance, $NA = 0.45$) was focused on the buffer surface in the Langmuir trough. Focusing was achieved by moving the optics rather than the trough. The image was recorded by charge-coupled device (CCD) camera (Pulnix, Sunnyvale, CA), viewed on computer and recorded by VCR (HS U69, Mitsubishi, Cypress, CA).

Fluorescence quenching experiments

To determine the vertical location of the disks with respect to the monolayer, we added $CoCl_2$ as an aqueous quencher to the subphase below monolayers labeled with fluorescent lipids. In each experiment, $CoCl_2$ was titrated into the subphase after the monolayer was compressed across the plateau to produce fluorescent disks. The total duration of each experiment was several hours. Experiments with CLSE, but not with DPPC/dchol, required intermittent compression during that time to maintain surface pressure constant. This additional compression decreased area by no more than 10%.

The quenching experiments used monolayers of CLSE and of DPPC/dchol 60/40 (mol:mol). For DPPC with 40% dchol, a subphase of plain water optimized the electrostatic interaction between the negatively charged

fluorescent probe and the positively charged cobalt ion. For CLSE, which contains anionic lipids, the experiment was performed on HSC, the usual calcium-containing buffer. With CLSE and for DPPC with 25% and 30% dchol, we consistently observed a decrease in the monolayer fluorescence as disks were produced by compression across the plateau. This decrease could be due either to self-quenching of the probe within the monolayer, or to repartitioning of the probe into the disks. Therefore, in the CLSE quenching experiment, the monolayer was compressed far enough onto the plateau to visualize the disks in FM, but not so far that the monolayer fluorescence dropped significantly.

Light scattering microscopy

The nucleation and growth of new phases in CLSE were studied using light scattering microscopy. Light from the BAM laser that scattered about the surface normal was collected by the same objective and CCD camera used in FM. Different filters placed in front of the CCD camera distinguished scattering from fluorescence. Rhodamine and FITC filters selected fluorescent and scattered light, respectively. Omission of any filter provided a composite contrast of FM and LSM.

The LSM employed here differed from one described by our group previously (Schief et al., 2000a,b) by the omission of an intensifier used in prior experiments to amplify the signal from the CCD camera. The sensitivity in the current studies was therefore lower by a factor of $\sim 10^4$. The boundaries between condensed domains and the surrounding liquid-expanded (LE) phase in DPPC monolayers, observed previously with LSM (Schief et al., 2000a), were not detected without the intensifier. The collapsed structures, however, were clearly evident.

RESULTS

Disks formed from CLSE and CLSE/cholesterol 80/20 (mol/mol)

Compression of monolayers containing CLSE produced π-A isotherms that rose smoothly to a plateau of relatively constant surface pressure (Fig. 1). Before reaching the plateau, FM demonstrated the previously described nonfluorescent domains and surrounding bright phase (Fig. 2 *A*). With the addition of scattering contrast, the monolayer appearance was similar (Fig. 2 *B*), except for a few bright individual scattering centers, apparent even in the absence of a monolayer, that correspond to nonlipid impurities detected regularly with LSM (Schief et al., 2000a).

At the onset of the plateau, new point scatterers emerged suddenly within the fluorescent phase (Fig. 2 *D*). These nuclei were undetectable by FM alone (Fig. 2 *C*). Further compression produced more scattering nuclei, and the fluorescent monolayer phase filled with point scatterers (Fig. 2 *F*), which then became detectable by FM (Fig. 2 *E*). With continued compression across the plateau, the nuclei grew into brightly fluorescent and strongly scattering disks with diameter ~ 1 μm (Fig. 2, *G* and *H*). The plateau in the isotherm therefore corresponds to the nucleation and growth of a new phase that forms only from LE regions of the monolayer, that is sufficiently distinct in thickness from the monolayer to scatter light, and that is sufficiently disordered to accommodate a lipid probe that has a low solubility in condensed phases.

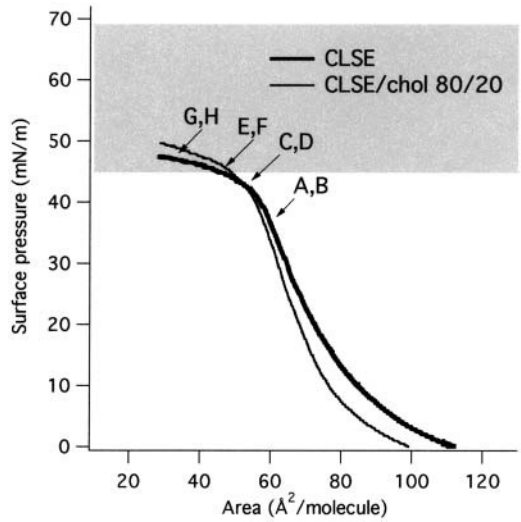

FIGURE 1 π-A isotherms for CLSE and CLSE/chol 80/20 (mol/mol). The gray shaded area denotes the physiological range of surface pressures that exist in the lungs (Horie and Hildebrandt, 1971; Schürch, 1982). Arrows indicate points at which images were obtained in Fig. 2. Temperature, 22°C; subphase, HSC.

The grayscale in BAM images, which is directly related to the optical thickness of visualized structures, provided a basis for determining the thickness of the collapsed disks. Because the lateral resolution of BAM is less than for FM or LSM, measurements with BAM required larger disks than those formed from CLSE. Reduction of the compression rate increased the disk size slightly (Fig. 4 *A*), but the addition of 20% cholesterol (mol:mol) produced a significantly greater enlargement (Fig. 3 *B*). π-A isotherms for the CLSE/cholesterol mixture were similar to curves for CLSE (Fig. 1), as were the nucleation and growth of structures evident by FM and LSM. The disks formed from CLSE/cholesterol did achieve the size necessary for visualization by BAM (Fig. 4 *A*).

Structures collapsed from DPPC/dchol mixtures

To gain additional information about the properties of the disks and the process by which they form, we developed a synthetic, compositionally simpler model system that would produce large disks. Based on the ability of added cholesterol to enlarge the disks from CLSE, we determined whether binary films of DPPC with various amounts of dchol would also collapse to form larger disks. We used dchol because of its greater stability than cholesterol and to avoid problems with oxidation at the air/water interface (Benvegnu and McConnell, 1993).

The compression isotherms for DPPC/dchol mixtures again contained plateaus consistent with collapse. In experiments with 80 and 100 mol % dchol, BAM showed that the collapsed structures were optically anisotropic crystals rather than disks (Fig. 5, *J–O*). For both mixtures, the plateau in the isotherm began with a cusp that suggested an activation

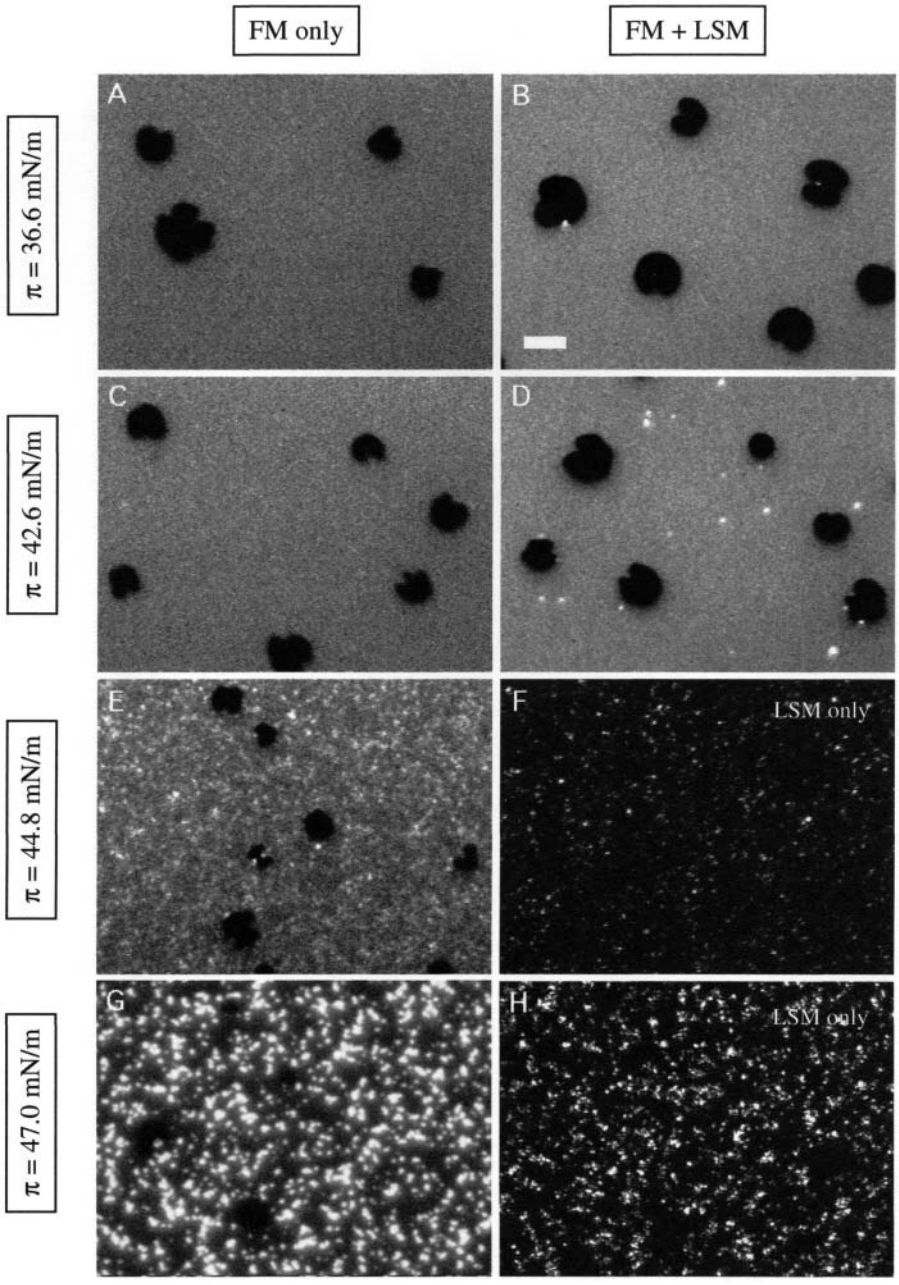

FIGURE 2 Visualization of the nucleation and growth of a three-dimensional phase from compressed monolayers of CLSE. Images were obtained using fluorescence microscopy (FM) and/or light scattering microscopy (LSM) (see Methods). The interface was illuminated with the BAM laser, which excites the fluorescent probe. Images *A*, *C*, *E*, and *G* show micrographs obtained using FM only (Rhodamine filter). Images *B* and *D* show fluorescence + scattering (no filter). Images *F* and *H* show scattering only (FITC filter). Images are displayed at the following conditions of (surface pressure [mN/m], molecular area [$Å^2$/phospholipid molecule]: *A* and *B*, (36.6, 59.9); *C* and *D*, (42.6, 52.8); *E* and *F*, (44.8, 45.3); *G* and *H*, (47.0, 32.1). Scale bar, 10 μm.

barrier to crystal nucleation. After compression beyond the cusp, BAM detected only crystallites. The large reflectivity of the crystals demonstrates that they are three-dimensional. These findings are consistent with previous reports of crystallization during collapse of mixed DPPC/cholesterol monolayers with as low as 66 mol % cholesterol (Worthman et al., 1997; Lafont et al., 1998).

For mixtures containing 25–60% dchol, compression across the collapse plateau formed disks that were intensely fluorescent by FM (Fig. 3) and brightly reflective by BAM (Fig. 5, *A–I*). Bright points appeared in BAM at the beginning of the plateau and grew with further compression into uniformly reflective disks with 10–500 μm diameters. The lack of any change in BAM contrast during rotation of an analyzer in the reflected beam indicated that the disks were optically isotropic, consistent with a fluid phase. Visual fields imaged with both microscopic methods showed a high correlation between fluorescence intensity and BAM gray-scale, both for partially and completely overlapping disks, and for the disks relative to the monolayer (Figs. 3 and 4). The fluorescence intensity of disks formed from unmodified CLSE, which were poorly resolved with the limited lateral resolution of BAM, was therefore used to judge their thickness qualitatively.

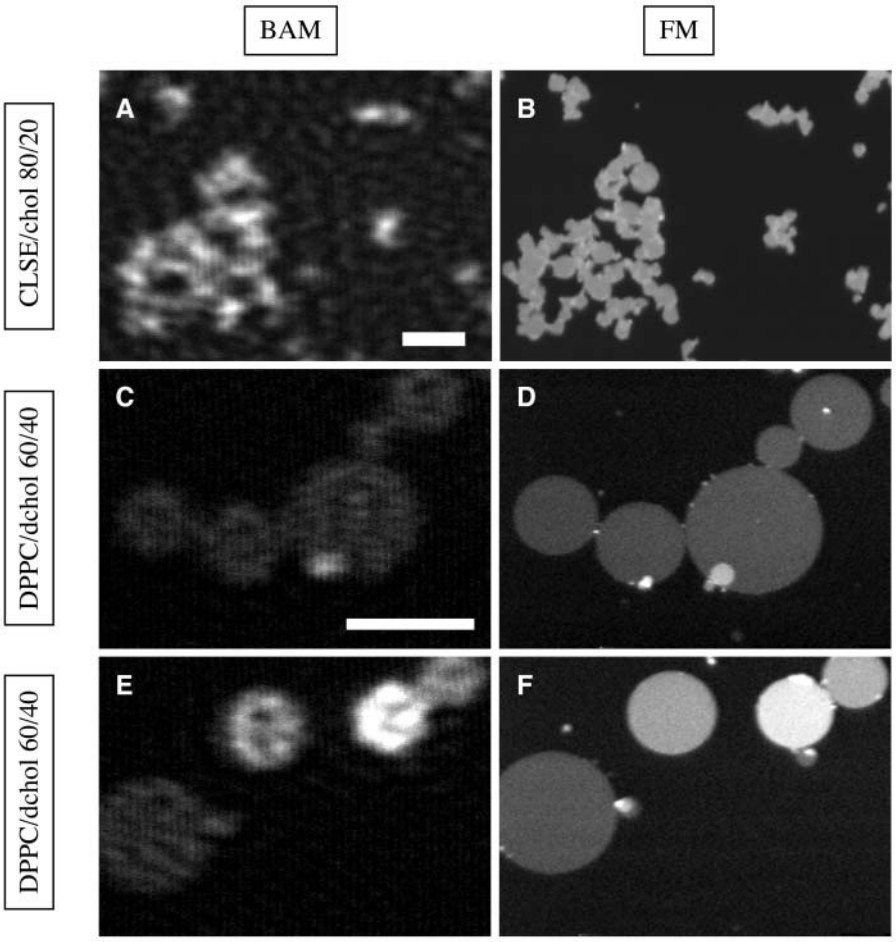

FIGURE 3 Simultaneous observation in Brewster angle microscopy (BAM) and FM of disks formed by compression of DPPC/dchol or CLSE/cholesterol monolayers. BAM micrographs in left column, FM in right column. Image pair (*A*, *B*) shows CLSE/chol 80/20 (mol/mol). Image pairs (*C*, *D* and *E*, *F*) show DPPC/dchol 60/40 (mol/mol). All films contained 0.5 mol % Rh-DPPE. Scale bars are 25 μm in *A* and 50 μm in *C*.

Thickness of disks

BAM grayscale provided a method for determining the thickness of disks relative to the monolayer for the structures collapsed from the DPPC/dchol mixtures and for the CLSE/cholesterol 80/20 (mol/mol). Because the disks were highly reflective, the unattenuated intensity from these structures frequently exceeded the dynamic range of the CCD camera. An extended grayscale was therefore constructed by rotating an analyzer in the reflected beam to reduce intensity in a predictable fashion (Fig. 6 *A*). Attenuated grayscales obtained at the different angles were then extrapolated to obtain the value expected at *p*-polarization (see Methods).

Grayscales measured on this extended scale for the clean interface, the monolayer, and overlapping disks were then compared with theoretical predictions based on a simple model. The model assumed that each disk had the refractive index of an individual monolayer and the thickness of an integral number of monolayers. Predicted reflectivities, calculated using Fresnel's equations extended for a stack of identical layers (Azzam and Bashara, 1977), were converted into grayscale values by identifying the grayscale measured for the buffer with a reflectivity of zero, and the grayscale for the monolayer with the reflectivity of that structure. A similar approach has been used previously to determine the relative thickness of structures collapsed from monolayers containing the liquid-crystal 4′-*n*-octyl-4-cyanobiphenyl (8CB) (de Mul and Mann, 1998). The isotropic structures observed in our studies, however, removed the requirement for anisotropic dielectric constants and allowed simpler calculations.

The extended grayscales measured for disks fit well with the thickness of three monolayers, consistent with a bilayer stacked on a monolayer (Fig. 6 *B*). For a double disk, the measured grayscale was intermediate between the values predicted for four and five monolayers. Because four layers would require exposure of either hydrophilic phospholipid headgroups to air or hydrophobic acyl chains to water, five monolayers, or two bilayers stacked on a monolayer, should be energetically more favorable (Fig. 6 *B*). We conclude that the disks for both CLSE and DPPC/dchol are bilayers adjacent to the interfacial monolayer, and that the stacked or overlapping disks are multiple bilayers.

Our approach required values for the physical thickness and refractive index of the base monolayer to calculate the grayscale for a multilayer stack. We used 2.5 nm and 1.5 for the thickness and refractive index, respectively. Because the curves were normalized to the grayscale of the monolayer,

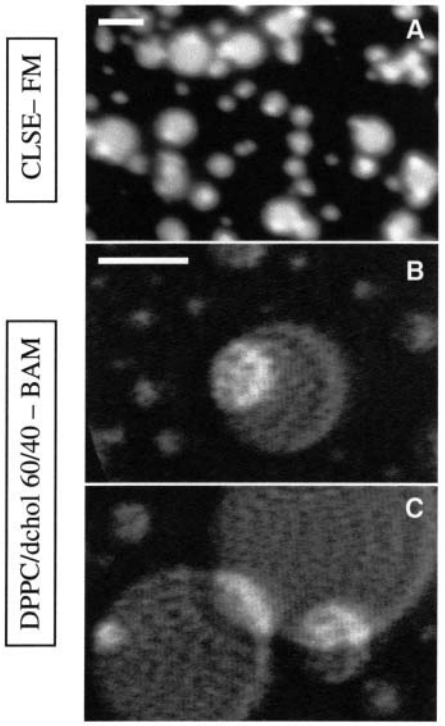

FIGURE 4 Representative micrographs of stacked or overlapping disks formed by compression of monolayers containing CLSE or DPPC/dchol 75/25 (mol/mol). (*A*) FM image of CLSE. (*B* and *C*) BAM images of DPPC/dchol. Brighter regions in BAM indicate greater thickness. Scale bar is 5 μm in *A*, and 50 μm in *B*.

the calculated curves were quite insensitive to these assumptions. For stacks of fewer than 10 identical monolayers, with physically reasonable refractive indices (1.4–1.7) and monolayer thicknesses (0.1–3.0 nm), the normalized reflectivity of a stack of identical monolayers varied by <5%.

Several more complicated models for the structure of the disks were also tested. Additional structural features included: 1), water layers of variable thickness (1–3 nm) between opposing headgroup regions; 2), different refractive indices and thicknesses for the headgroup and tail regions ($1.4 < n_{head} < 1.5$, $1.4 < n_{tail} < 1.5$, $d_{head} = 0.7$ nm, and $d_{tail} = 1.3$ nm); and 3), reduced physical thickness because of interdigitation between opposing tail regions. These features were tested alone and in combinations for disks protruding into the air and into the water. Although in some cases reflectivities predicted by the simplest and more complex models differed for the double disks, values predicted for the single disks were unaffected.

Vertical location of the disks with respect to the monolayer

To address the question of whether the CLSE and DPPC/dchol disks were located above or below the monolayer, or whether some were above and others below (Fig. 7 *A*), we used a fluorescence quenching experiment. The fluorescent probe (Rh-DPPE) has a fluorophore attached to the polar headgroup. We therefore determined the extent to which the aqueous quencher Co^{2+} (Homan and Eisenberg, 1985; Morris et al., 1985) could alter the fluorescence of the collapsed disks. We assumed that the fluorophores would be inaccessible to quenchers in the subphase only if located in bilayer disks above the monolayer (Fig. 7 *A*). For disks on the aqueous side of the monolayer, fluorescence from all three layers would fall. For disks above the monolayer, the quencher would affect only the monolayer itself, and when viewed from above, intensity from the disks would fall only to the same extent as the surrounding film.

Quenching experiments were performed separately for CLSE and for DPPC/dchol 60/40 (mol/mol). In each experiment, $CoCl_2$ was titrated into the subphase after the monolayer was compressed across the collapse plateau to produce fluorescent disks. For DPPC/dchol and CLSE, a comparison of FM images taken before the addition of quencher and after equilibration with progressively higher quencher concentrations showed qualitatively that although the fluorescence from both monolayer and disks decreased, the disks remained brighter (Fig. 7 *B*). Quantitative analysis showed that the intensity of the monolayer and the disks decreased in parallel with added quencher (Fig. 7 *C*). The decreased fluorescence in both cases could then be explained by quenching restricted to the monolayer.

In a control experiment, the DPPC/dchol monolayer was exposed to the fluorescence lamp continuously for 4 h, well beyond the total exposure of less than an hour used in the quenching experiments. Quantitative analysis of fluorescence intensities from the control experiment showed no decrease in intensity for the monolayer or the disks over the duration of the experiment (Fig. 7 *C*). The control experiment excluded systematic causes for the decreasing intensity measured in the presence of quencher such as bleaching, a drop in lamp intensity, or drift of camera gain or offset. The disks were therefore inaccessible to aqueous quencher, consistent with their location above the monolayer.

We also verified with LSM, which visualized the disks by light scattered from their edges (Schief et al., 2000a), that no completely quenched disks were present at the interface. All disks visible in LSM were also visible in FM (data not shown). Neither fluorescent disks nor particles were detected floating beneath the monolayer during compression across the high-pressure plateaus of fluorescently labeled CLSE or DPPC/dchol monolayers. A few fluorescent particles were detected in the subphase during expansion of CLSE monolayers after disk formation, indicating that some of the disks in CLSE may form underneath the monolayer. Our results, however, generally fit better with disks that reside above the monolayer.

Dynamics of disk formation

Several experiments provided insight into the dynamic

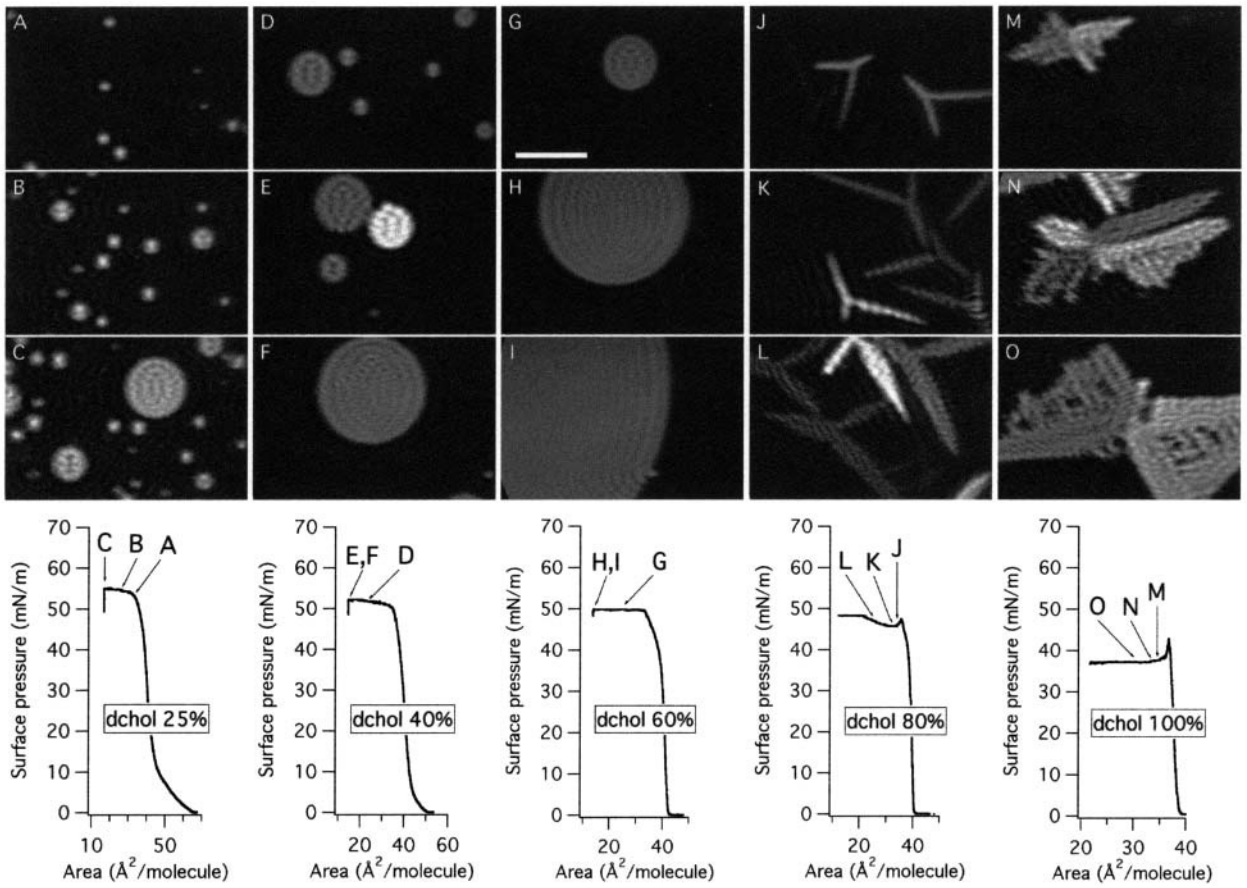

FIGURE 5 Nucleation and growth of collapsed disks from DPPC/dchol monolayers. Images (*top*) were recorded by BAM at the points indicated on the isotherms (*below*). BAM intensities were reduced by rotation away from *p*-polarization of an analyzer in the reflected beam. Scale bar, 50 μm.

processes of collapse. First, we found that nucleation of individual disks could proceed as a sudden, rapid event, and that disks did not all nucleate simultaneously at the onset of collapse. During compression across the plateau, we observed several times the sudden emergence of a disk tens of microns in diameter surrounded by previously nucleated disks. The nucleation sites within the monolayer appeared to be randomly distributed. Fig. 8 shows the time sequence of one such sudden nucleation event. The new disk grew to a diameter of roughly 5 μm within <5 s. Individual micrographs also tended to include disks with a broad range of sizes, consistent with structures that grew after nucleation that occurred progressively rather than simultaneously at a single point in time (Figs. 3–5).

Dynamics of disk fusion

Once formed, the disks were generally stable, and fusion between disks was rare. Disks were more likely to form multiple bilayers stacked on top of each other than larger single-bilayer disks. A variety of stacking scenarios occurred, including small disks completely overlapping larger disks (Fig. 4 *B*), concentric bilayer stacks of equal diameters (Fig. 3, *E* and *F*; Fig. 5 *E*), and single bilayer disks that partially overlapped (Fig. 4 *C*). Two or more disks also often attached without fusing, forming an assembly or chain of disks (Fig. 3, *A* and *B* for CLSE/cholesterol; Fig. 3, *C* and *D*, for DPPC/dchol). Several such chains remained stable without fusing for 10 min or more. Fusion occurred occasionally. Fig. 9 shows two adjacent disks in a sample of DPPC/dchol that were followed for approximately 2 min before fusion by tracking the disks with the FM objective. Once fusion began, the two disks fused completely within 1.3 s into a single large disk.

Dynamics of stacking and bending of multibilayer disks

Further experiments that tracked individual structures in the moving monolayer demonstrated details of the dynamic processes involved in collapse. Additional layers often grew from a disk through a brightly fluorescent spot (Fig. 10 *A*). The increased brightness of the spot relative to the other disks suggested greater thickness. A time series recorded during monolayer compression showed the growth of a second layer, indicated by the brighter fluorescence than for the original disk, on a disk from this thicker spot (Fig. 10,

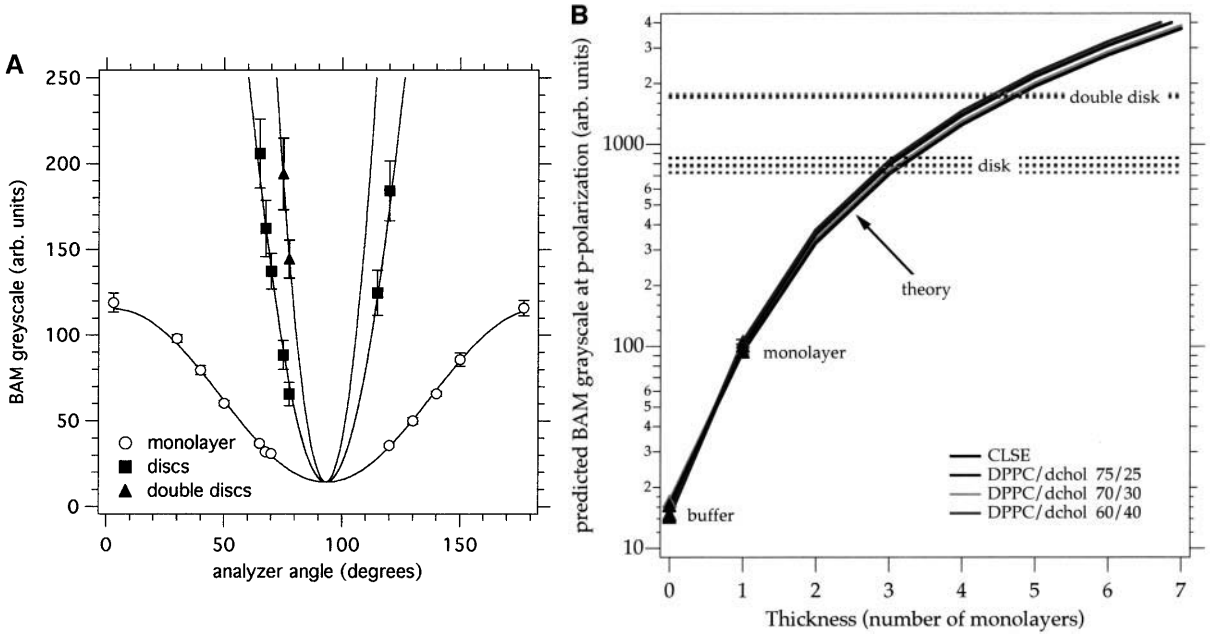

FIGURE 6 Determining the relative optical thickness of disks. (*A*) BAM grayscale versus analyzer angle for the monolayer, single disks, and double disks (stacked or overlapping) in one typical experiment with DPPC/dchol 75/25 (mol/mol). Each measured grayscale represents the mean of a Gaussian fit to a grayscale histogram taken from the monolayer, disks, or double disks in several images. Error bars give the probable error in the mean (Bevington and Robinson, 1992). α_p, the position of p-polarization, here is 3°, and g_0, the grayscale minimum at s-polarization, is 15 arbitrary units. With g_0 and α_p determined from values for the monolayer, Eq. 1 can be solved using measured $g(\alpha)$ to determine g_p, the extended grayscale that would occur at $\alpha = \alpha_p$. (*B*) Predicted variation of extended BAM grayscale with thickness. Calculations assumed that collapsed structures had the same refractive index as monolayers, and that the increment in grayscale produced by that particular monolayer corresponded to its reflectivity. Thickness is expressed relative to an individual monolayer. Horizontal dashed lines give extended grayscale values measured for disks and double disks.

B–F). Throughout the compression, the intensely fluorescent spot from which the second disk emerged remained remarkably bright and fixed on the edge of the large disk without movement along its perimeter. The smaller disk appeared to rotate around the spot (Fig. 10, *D* and *E*). These observations suggest that the growth of the second disk resulted from flow of material through the spot.

When the smaller disk grew beyond the edge of the larger one, it bent over that edge (Fig. 10, *C*, *D*, and *F*), leaving part of the smaller disk with the same fluorescence intensity as the larger one. The large disk then fused with that portion of the smaller one (Fig. 10, *G–I*). Both disks, presumably driven by line tension, then rearranged into circular forms.

Dynamics of disk reinsertion

Collapse of DPPC/dchol mixtures to form disks was reversible. On expansion, the disks shrank either from interior holes (Fig. 11) or from a point on the disk's edge (Fig. 12). A time sequence of a single disk reincorporating into the monolayer showed that the disk could deflate from a single bright point on its edge (Fig. 12), suggesting movement of constituents through a connection to the underlying monolayer. With the slow expansion rates of 1–2 Å^2/(molecule × minute) employed in these studies, ~90% of the material in DPPC/dchol disks reincorporated into the monolayer above surface pressures of ~30 mN/m. If expanded to zero surface pressure, the remaining material (<10%) generally reinserted into the film.

Expansion of CLSE showed behavior similar to DPPC/dchol. The fluorescent disks and aggregate structures shrank and became dimmer (Fig. 13, *A* and *B*), completely disappearing in FM at ~30 mN/m (Fig. 13 *C*). LSM confirmed that the number of scatterers decreased significantly with expansion to 30 mN/m, although some persisted to zero surface pressure before disappearing (Fig. 13 *D*).

Although microscopy demonstrated that the two-to-three dimensional phase transition could be completely reversed, the π-A isotherms for both CLSE and DPPC/dchol during both expansion and recompression showed significant hysteresis (not shown). The virtually complete reinsertion of the disks into the monolayer indicated that collapse of material into these structures could not explain the hysteresis. An alternative explanation for hysteresis is that lipid molecules may deposit onto the Teflon ribbon barrier of the Langmuir trough. Film leakage or creep onto Teflon barriers occurs at low surface tensions and has been documented previously using radioactively labeled phospholipids (Goerke and Gonzales, 1981). The isotherm plateau itself is not an artifact of leakage. Slow compression of CLSE monolayers on the continuous interface of a leak-proof captive bubble confirms the existence of a long plateau at ~46 mN/m (Crane

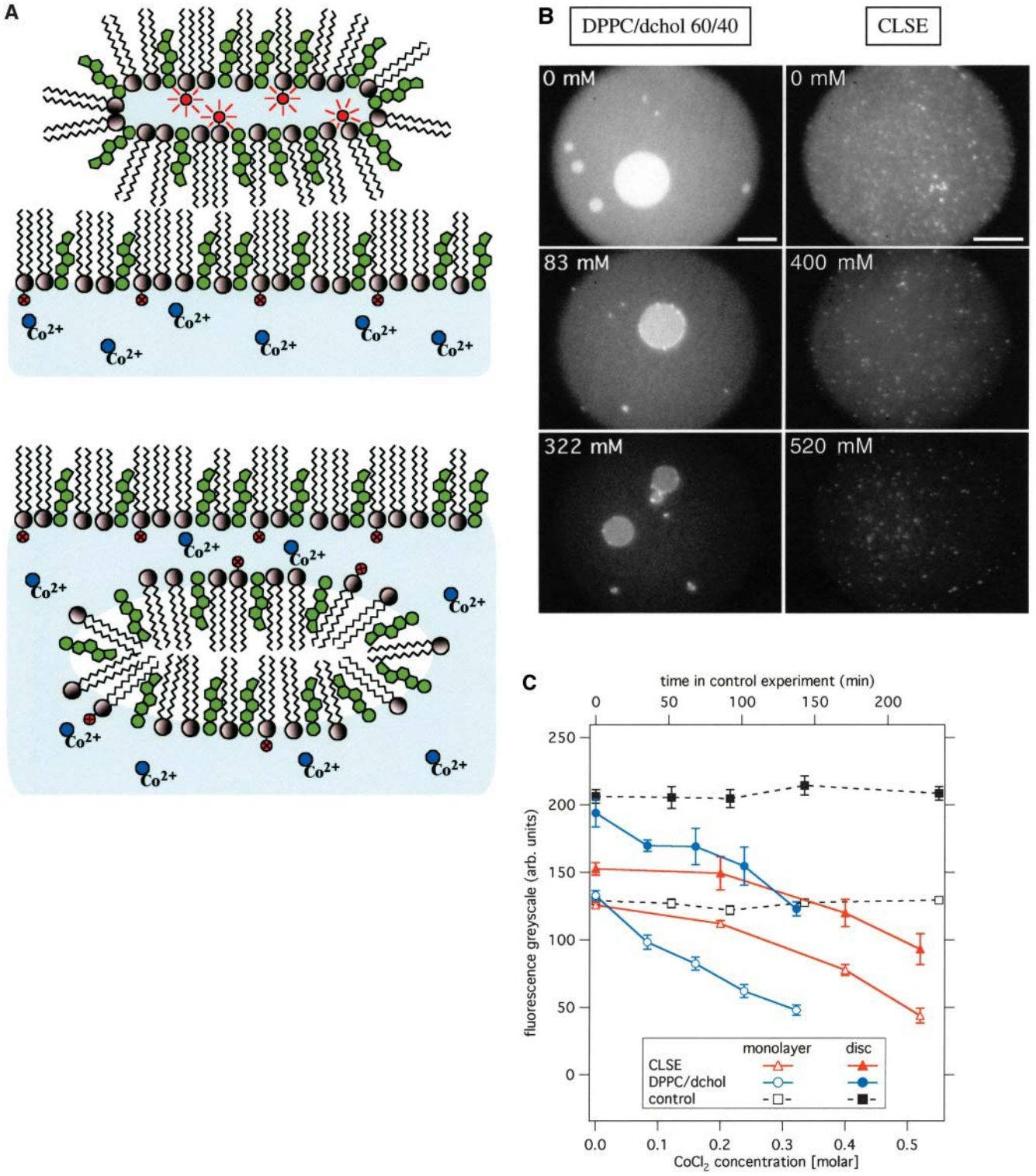

FIGURE 7 Fluorescence quenching of monolayer and collapsed disks. (*A*) Concept of experiment. If the bilayer disks rest above the monolayer, the fluorescent headgroups in the disks will be inaccessible to the quenching cobalt ions in the aqueous subphase. If the disks are attached beneath the monolayer, their structure would be inverted, with the polar headgroups exposed to the subphase and quenched by the cobalt. Fluorescence from the monolayer in both cases should be quenched. (*B*) FM images of monolayer and disks recorded at increasing concentrations of $CoCl_2$ for DPPC/dchol 60/40 (mol/mol) at 52 mN/m (*left column*) and for CLSE at 47 mN/m (*right column*). Images are labeled with quencher concentration. The subphase contained HSC for CLSE and water for DPPC/dchol. Scale bar is 25 μm in both columns. (*C*) Fluorescence intensities for monolayer and disks plotted versus quencher subphase concentration (*solid lines, bottom axis*) for both CLSE and DPPC/dchol 60/40 (mol/mol). Also shown are the intensities of monolayer and disks for DPPC/dchol 60/40 plotted versus time (*dashed line, top axis*) in the absence of quencher.

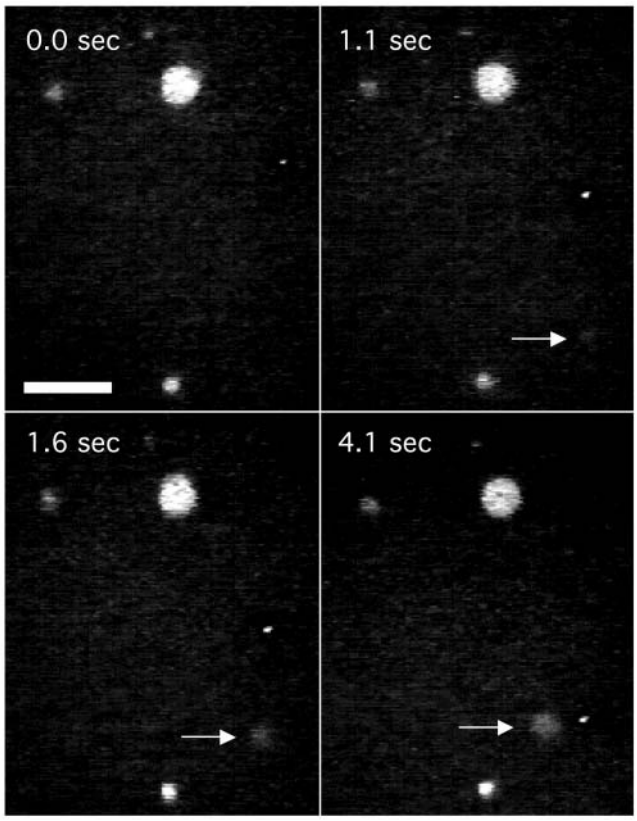

FIGURE 8 FM time series of disk nucleation in DPPC/dchol 75/25 (mol/mol). Images were recorded at the times after the initial micrograph indicated on each image. Scale bar, 10 μm.

and Hall, 2001), consistent with the collapsed structures observed microscopically here.

DISCUSSION

Structures collapsed from pulmonary surfactant

The most remarkable aspect of pulmonary surfactant's behavior in situ is its ability to avoid collapse for prolonged periods at surface pressures well above the equilibrium spreading pressure (Horie and Hildebrandt, 1971; Schürch, 1982). The microscopic studies reported here demonstrate the three-dimensional structures that coexist in vitro with the two-dimensional film. They establish mechanisms by which collapse occurs during quasi-equilibrium compressions, and provide the basis for understanding the process that must be circumvented in situ. Prior reports have demonstrated a variety of structures that monolayers can form when they collapse. Simple model systems of pulmonary surfactant have shown two structures in particular that depend on the conditions under which the films are compressed. Films can buckle and form folds that extend far into the subphase, or they can bud to form disks (Gopal and Lee, 2001). Factors that favor more fluid structures, such as higher temperatures,

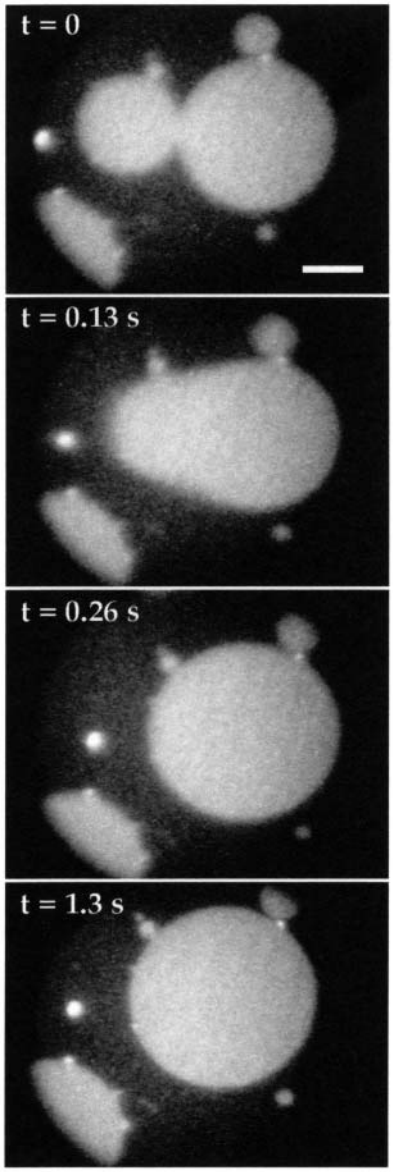

FIGURE 9 Fusion of disks collapsed from DPPC/dchol 60/40 (mol/mol) monolayers. Fluorescence micrographs show a temporal sequence obtained after tracking two adjacent disks for ~2 min. Similar events were observed without prior extended exposure to the fluorescence lamp. Pairs or groups of adjacent disks more commonly failed to fuse during tracking for more than 10 min. Scale bar, 25 μm.

promote the formation of disks. We show here that at subphysiological temperatures, the complete biological mixture collapses to form disks. Higher temperatures would presumably accentuate that tendency. We conclude that the formation of disks represents the mode of collapse relevant to the native mix of surfactant constituents.

DPPC/dchol replicates the collapse of the surfactant extracts in several respects. When overcompressed, films containing DPPC/dchol or CLSE both form disks that have the thickness of two monolayers, and that appear inaccessible to quencher in the aqueous phase, consistent with their

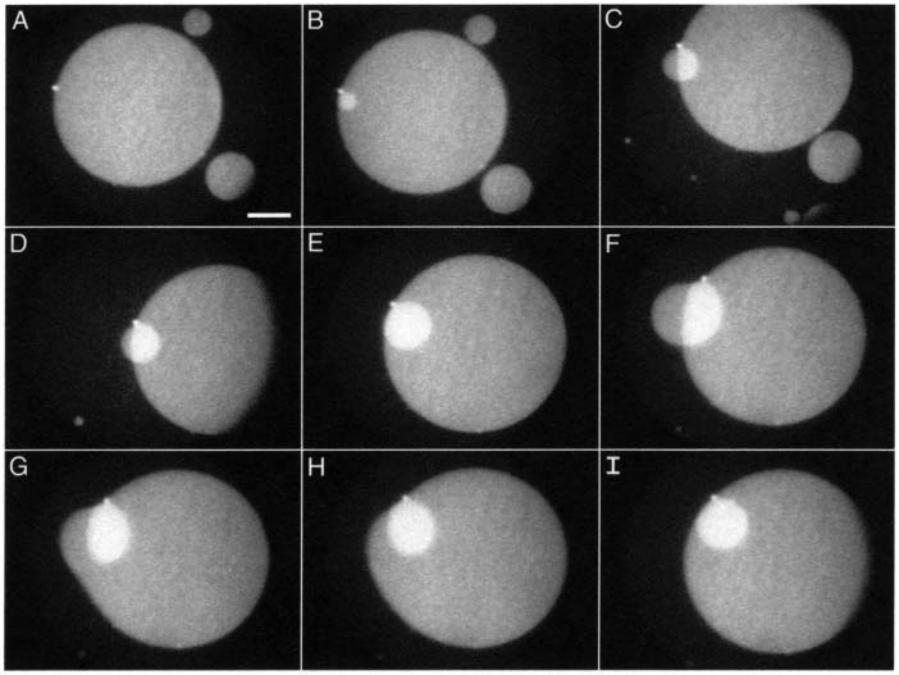

FIGURE 10 Growth of a stacked disk. Temporal sequence of fluorescence micrographs show structures formed from monolayers of DPPC/dchol 60/40 (mol/mol) at 52 mN/m. Images were recorded at the following times after the initial image: (*A*) 0.0 s; (*B*) 15.0 s; (*C*) 68.8 s; (*D*) 73.7 s; (*E*) 87.8 s; (*F*) 133.0 s; (*G*) 133.1 s; (*H*) 133.2 s; and (*I*) 133.4 s. Scale bar, 50 μm.

location above the monolayer. In both cases, further compression of the films produces additional disks stacked on the initial structures well before they grow to confluence. The disks that collapse from both films attach to form chains but rarely fuse. They also reincorporate into the expanding monolayer. Although some experiments concerning the details of these processes benefited from the larger disks generated from CLSE with added cholesterol, these similar behaviors occurred for DPPC/dchol and for the unaltered surfactant extracts. DPPC/dchol mixtures therefore provide an appropriate model system for studying the mechanisms by which surfactant monolayers collapse.

Liquid-crystalline collapse

Several compounds that form smectic liquid-crystal bulk phases collapse from monolayers into structures similar to the ones observed here. 8CB, the compound studied in most detail (Xue et al., 1992; de Mul and Mann, 1994; Friedenberg et al., 1994; Fang et al., 1997), also forms bilayer disks (de Mul and Mann, 1998), the behavior of which shows many of the same distinct features shown for CLSE and DPPC/dchol. The disks pack into close proximity but rarely fuse (Friedenberg et al., 1994). Their circular shape, optical isotropy, and rapid reconfiguration all indicate a fluid structure (de Mul and Mann, 1994; Friedenberg et al., 1994). The disks stack into multiple layers before forming a single confluent layer (de Mul and Mann, 1994), and frequently reinsert into an expanding film from the center of the disk, resulting in central holes (Friedenberg et al., 1994). Hydrated phospholipids themselves are liquid-crystals, and in these multiple respects, their behavior resembles that of at least some other compounds that form smectic bulk phases.

A key aspect of this form of collapse is that the monolayer flows continuously into the collapsed phase. This movement through a connecting structure has been proposed previously

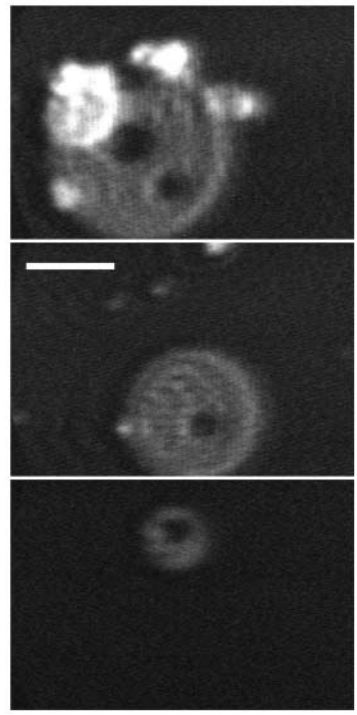

FIGURE 11 Reincorporation of collapsed disks during expansion of DPPC/dchol 60/40 (mol/mol). BAM images showing different disks from which material is lost by the formation of interior holes. Scale bar, 50 μm.

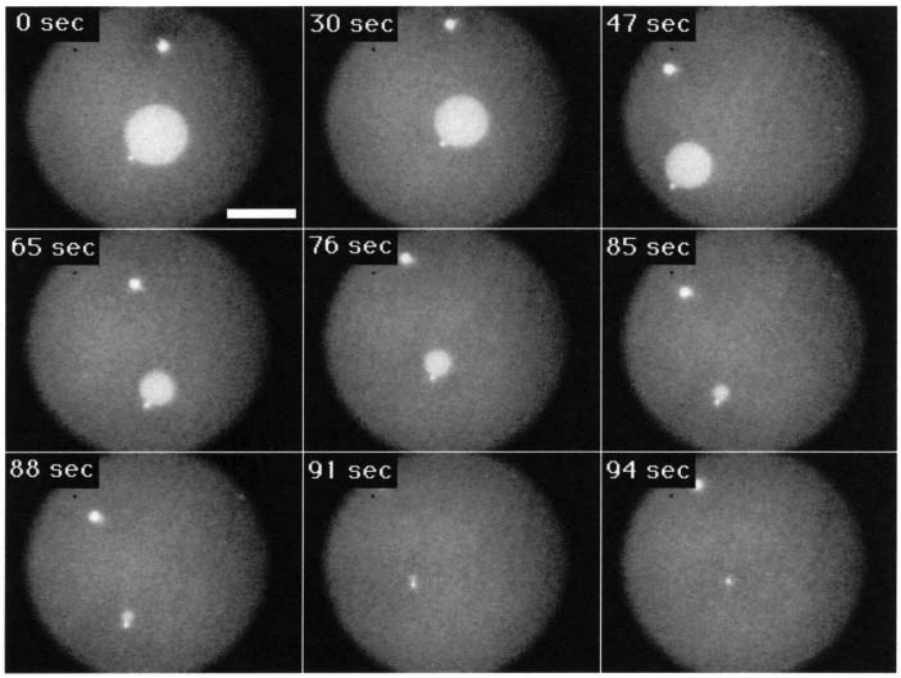

FIGURE 12 Reincorporation of a collapsed disk into a monolayer of DPPC/dchol 60/40 (mol/mol) during expansion. The sequence of fluorescence micrographs shows that the disk deflates from the single bright point on its edge. Scale bar, 50 μm.

(de Mul and Mann, 1994), but the demonstration of distinct stalks from which the disks grow in our studies provides perhaps the most conclusive evidence. This process then differs at least in detail from the mechanism considered previously for compounds that collapse to form bulk liquids or crystals. For those cases, monolayers collapse by nucleation of a bulk phase that grows by diffusion of individual constituents across the boundary between the two- and three-dimensional phases (Smith and Berg, 1980). Specific models have considered the kinetics by which additional constituents add to the base or edge of a collapsed lens, a hemispherical droplet, or a cylindrical disk (Vollhardt and Retter, 1991). Our results indicate that these models represent a process different from the collapse of pulmonary surfactant.

Prior reports with compounds such as 8CB have suggested that the collapsed disks formed above the monolayer, away from the aqueous subphase (Xue et al., 1992; de Mul and Mann, 1994; Friedenberg et al., 1994; Fang et al., 1997). For the systems studied here, the fluorescence quenching experiments strongly support that direction of collapse. The behavior of these disks differs from a number of systems that collapse by forming folds which extend hundreds of microns into the aqueous phase (Lipp et al., 1998; Gopal and Lee, 2001). Our interpretation does assume that fluorescent lipids labeled at the headgroup would be inaccessible to aqueous quenchers only if located above the monolayers. For a bilayer disk formed below the monolayer, we assume that cobalt added after collapse would penetrate the gap between monolayer and disk and eliminate fluorescence from lipid probe located there. Given the limits of close approach for two bilayers (Rand and Parsegian, 1989; McIntosh and Simon, 1994; Israelachvili and Wennerstrom, 1996) and the evidence that divalent cations can penetrate that separation (McIntosh et al., 1990), this assumption seems eminently reasonable.

The behavior of the disks emphasizes a factor inherent in their mechanism of collapse. The sliding of disks along the monolayer introduces a frictional resistance to growth of the multilayered phase that would be absent during the diffusion of individual constituents into a collapsed liquid droplet or crystal. Such a resistance to movement could contribute both to the low frequency with which adjacent disks fuse, and to the stacking of disks rather than growth of a single layer to confluence. Our results indicate that friction is not a major limitation of fusion. On the rare occasions when fusion occurs, reconfiguration into a new circular shape is rapid. For the stacking of disks, that process represents a balance between the relative energetics of extending an initial disk as opposed to the growth of smaller superimposed structures. The frequency with which stacked disks occur indicate that these processes quickly become energetically similar. Friction, along with factors such as line tension, could be a significant determinant of that balance, and of the manner in which collapse progresses.

Role of cholesterol

The effect of dchol on DPPC monolayers is dramatic. DPPC by itself reaches and sustains surface pressures approaching 70 mN/m. Buds form from the monolayer at lower surface pressures, but although they become more numerous at higher pressures, they fail to extend laterally into the fully collapsed bilayer disks (Schief et al., 2000a). Cholesterol increases the intrinsic curvature and lowers the bending

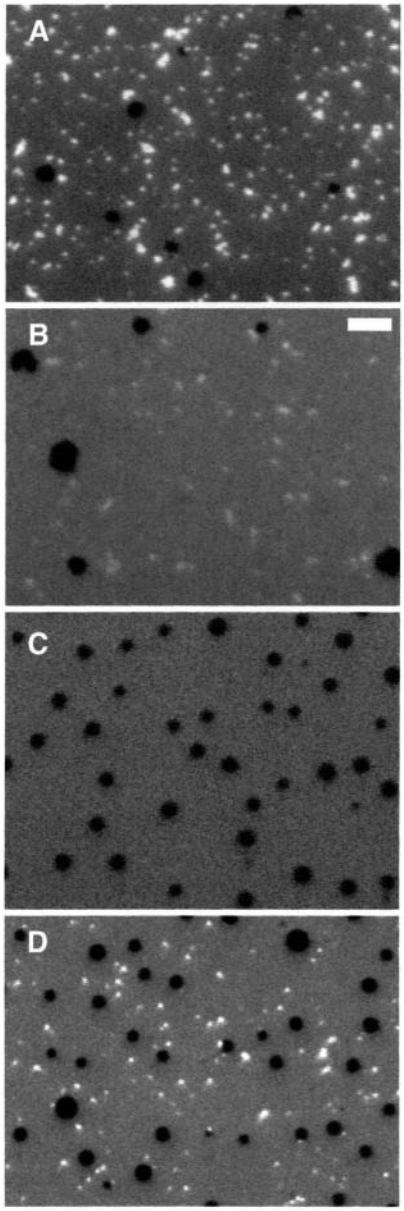

FIGURE 13 Reincorporation of CLSE disks during expansion. Fluorescence micrographs in *A*, *B*, and *C* were recorded at [surface pressure (mN/m), molecular area (Å^2/phospholipid molecule)] of [44.5, 36.2]; [39.4, 38.5]; and [1.7, 83.3]. Image *D* is a simultaneous FM and LSM image at [1.7, 83.3]. Scale bar, 10 μm.

energy of phospholipid structures (Chen and Rand, 1997). Formation of collapsed disks requires that the monolayer bends, and we presume that the extension of nascent buds, which form in DPPC alone, into bilayer disks results from dchol's effect on bending energy. The lower surface pressure at which collapse occurs with higher dchol content would reflect the same effect.

The tendency of cholesterol to facilitate collapse, demonstrated here and previously (Hildebran et al., 1979; Notter et al., 1980), should have physiological consequences. Cholesterol is the constituent of pulmonary surfactant for which it is best established that physiological factors produce a variation of levels. Swimming rats (Orgeig et al., 1995) and cold lizards (Daniels et al., 1990) both increase the relative amounts of cholesterol in their surfactant. The benefits of these changes have been explained in terms of alterations in the spreading of adsorbed material. Cholesterol tends to disrupt solid structures, whether gel phase in bilayers or the condensed phase in monolayers, that might occur in phospholipid mixtures rich in constituents such as DPPC that melt above body temperature. The more fluid structures that result from cholesterol's effects may adsorb more rapidly. Our results reinforce, however, the previous finding that better spreading should come at the cost of a greater tendency to collapse.

Compositional implications

The mechanism of collapse illustrated here has specific implications concerning the composition of the material excluded from the film, and for the function of pulmonary surfactant. The flow of an intact monolayer into the third dimension should carry with it all constituents in the local region where collapse occurs. The composition of the excluded material should then equal that of the monolayer phase from which it is formed. The behavior of the different DPPC/dchol mixtures is consistent with that hypothesis. Films containing only dchol collapse to form crystals, and at a much lower surface pressure than DPPC alone. If constituents collapsed from the mixed film individually, then material excluded from all of the DPPC/dchol monolayers should form similar crystals. The disks observed with $\leq$60% dchol and the crystals seen with 80% dchol, which are distinct from the structures formed by pure dchol, indicate that the more fluid constituent is not excluded as a single component, and fit with flow of the intact monolayer into the collapsed disks.

These results place specific constraints on how the composition of pulmonary surfactant can change in the lung. The classical model of surfactant function contends that only a condensed film can replicate the prolonged metastability at high surface pressures observed in situ (Clements, 1977; Bangham et al., 1979). Because DPPC is the only surfactant constituent that at physiological temperatures forms the condensed phase in single component monolayers, the classical model also holds that relative to the material secreted by the type II pneumocyte, the functional film in the lung must be greatly enriched in DPPC (Clements, 1977; Bangham et al., 1979). The mechanism originally proposed to explain this refinement was selective exclusion, or squeeze-out, of constituents other than DPPC at the equilibrium spreading pressure (Watkins, 1968; Clements, 1977; Bangham et al., 1979). Liquid-crystalline collapse, in which all constituents of a region flow together from the monolayer, ties selective exclusion directly to phase behavior. The proposed enrichment in DPPC would occur only to the extent that DPPC and

the other constituents segregate into different phases that have different stabilities.

Although surfactant films satisfy some of these requirements, our results here and elsewhere generally disagree with the model. Separate phases can coexist in films containing partial (Discher et al., 1999a,b; Piknova et al., 2001) or complete (Discher et al., 1996; Nag et al., 1998) extracts of pulmonary surfactant. For the complete set of phospholipids purified from CLSE, the condensed phase contains essentially pure DPPC, with the other compounds restricted to the surrounding film (Discher et al., 1999). The similar microscopic characteristics by FM and BAM of the condensed phase for CLSE suggests a similar composition. Our results here also show the required differential stability between the two phases, with collapse occurring only from the LE phase. At 37°C, however, the extent of phase separation is minimal (Discher et al., 1996). For CLSE, the condensed phase at 45 mN/m occupies, at most, a few percent of the interfacial area (Discher et al., 1996). Even if the condensed phase contains only DPPC, most of that compound must reside in the surrounding film. The collapse of surfactant constituents collectively rather than individually therefore complements the prior studies to argue that any compositional refinement by selective exclusion must be quite limited.

SUMMARY

Our results suggest that of the multiple structures which different monolayers form when supercompressed, pulmonary surfactant collapses by the same mechanism as other compounds that form smectic liquid-crystal bulk phases. Binary mixtures of DPPC/dchol replicate this form of collapse in multiple respects, and provide a simple model system for studying this process. The continuous flow of the monolayer into collapsed disks provides specific constraints that may contribute to understanding how pulmonary surfactant avoids collapse in the small air spaces of the lungs.

The authors thank Dr. Edmund Egan of ONY for providing CLSE, and Julia Hall for careful preliminary observations on the dynamics of collapsed structures.

These studies were supported by grants from the National Institutes of Health (HL 03502 and 60914), the Whitaker Foundation, and the American Lung Association of Oregon.

REFERENCES

Amrein, M., A. von Nahmen, and M. Sieber. 1997. A scanning force and fluorescence light microscopy study of the structure and function of a model pulmonary surfactant. *Eur. Biophys. J. Biophys. Lett.* 26:349–357.

Azzam, R. M. A., and N. M. Bashara. 1977. Ellipsometry and Polarized Light. North-Holland Publishing, Amsterdam, The Netherlands.

Bangham, A. D., C. J. Morley, and M. C. Phillips. 1979. The physical properties of an effective lung surfactant. *Biochim. Biophys. Acta*. 573: 552–556.

Bastacky, J., C. Y. Lee, J. Goerke, H. Koushafar, D. Yager, L. Kenaga, T. P. Speed, Y. Chen, and J. A. Clements. 1995. Alveolar lining layer is thin and continuous: low-temperature scanning electron microscopy of rat lung. *J. Appl. Physiol.* 79:1615–1628.

Benvegnu, D. J., and H. M. McConnell. 1993. Surface dipole densities in lipid monolayers. *J. Phys. Chem.* 97:6686–6691.

Bevington, P. R., and D. K. Robinson. 1992. Data Reduction and Error Analysis for the Physical Sciences. McGraw-Hill, New York.

Chen, Z., and R. P. Rand. 1997. The influence of cholesterol on phospholipid membrane curvature and bending elasticity. *Biophys. J.* 73:267–276.

Clements, J. A. 1977. Functions of the alveolar lining. *Am. Rev. Respir. Dis.* 115:67–71.

Crane, J. M., and S. B. Hall. 2001. Rapid compression transforms interfacial monolayers of pulmonary surfactant. *Biophys. J.* 80:1863–1872.

Daniels, C. B., H. A. Barr, J. H. Power, and T. E. Nicholas. 1990. Body temperature alters the lipid composition of pulmonary surfactant in the lizard *Ctenophorus nuchalis*. *Exp. Lung Res.* 16:435–449.

de Mul, M. N. G., and J. A. Mann. 1994. Multilayer formation in thin-films of thermotropic liquid-crystals at the air-water interface. *Langmuir.* 10:2311–2316.

de Mul, M. N. G., and J. A. Mann. 1998. Determination of the thickness and optical properties of a Langmuir film from the domain morphology by Brewster angle microscopy. *Langmuir.* 14:2455–2466.

Discher, B. M., K. M. Maloney, W. R. Schief, D. W. Grainger, V. Vogel, and S. B. Hall. 1996. Lateral separation of interfacial domains in films of pulmonary surfactant. *Biophys. J.* 71:2583–2590.

Discher, B. M., K. M. Maloney, D. W. Grainger, C. A. Sousa, and S. B. Hall. 1999a. Neutral lipids induce critical behavior in interfacial monolayers of pulmonary surfactant. *Biochemistry.* 38:374–383.

Discher, B. M., W. R. Schief, V. Vogel, and S. B. Hall. 1999b. Phase separation in monolayers of pulmonary surfactant phospholipids at the air-water interface: composition and structure. *Biophys. J.* 77:2051–2061.

Fang, J. Y., C. M. Knobler, and H. Yokoyama. 1997. Layer growth in collapsed liquid-crystal monolayers studied by scanning force microscopy. *Physica A.* 244:91–98.

Fontaine, P., J. Daillant, P. Guenoun, M. Alba, A. Braslau, J. W. Mays, J. M. Petit, and F. Rieutord. 1997. Spontaneous buckling induced by the adsorption of charged copolymers at the air-water interface. *J. Phys. II.* 7:401–407.

Friedenberg, M. C., G. G. Fuller, C. W. Frank, and C. R. Robertson. 1994. Formation of bilayer disks and two-dimensional foams on a collapsing/expanding liquid-crystal monolayer. *Langmuir.* 10:1251–1256.

Goerke, J., and J. Gonzales. 1981. Temperature dependence of dipalmitoyl phosphatidylcholine monolayer stability. *J. Appl. Physiol.* 51:1108–1114.

Gopal, A., and K. Y. C. Lee. 2001. Morphology and collapse transitions in binary phospholipid monolayers. *J. Phys. Chem. B.* 105:10348–10354.

Hénon, S., and J. Meunier. 1991. Microscope at the Brewster angle: direct observation of first-order phase transitions in monolayers. *Rev. Sci. Instr.* 62:936–939.

Hildebran, J. N., J. Goerke, and J. A. Clements. 1979. Pulmonary surface film stability and composition. *J. Appl. Physiol.* 47:604–611.

Homan, R., and M. Eisenberg. 1985. A fluorescence quenching technique for the measurement of paramagnetic ion concentrations at the membrane/water interface. Intrinsic and X537A-mediated cobalt fluxes across lipid bilayer membranes. *Biochim. Biophys. Acta.* 812:485–492.

Hönig, D., and D. Möbius. 1991. Direct visualization of monolayers at the air-water interface by Brewster angle microscopy. *J. Phys. Chem.* 95:4590–4592.

Horie, T., and J. Hildebrandt. 1971. Dynamic compliance, limit cycles, and static equilibria of excised cat lung. *J. Appl. Physiol.* 31:423–430.

Israelachvili, J., and H. Wennerstrom. 1996. Role of hydration and water structure in biological and colloidal interactions. *Nature*. 379:219–225.

Kramer, A., A. Wintergalen, M. Sieber, H. J. Galla, M. Amrein, and R. Guckenberger. 2000. Distribution of the surfactant-associated protein C within a lung surfactant model film investigated by near-field optical microscopy. *Biophys. J*. 78:458–465.

Lafont, S., H. Rapaport, G. J. Somjen, A. Renault, P. B. Howes, K. Kjaer, J. Als-Nielsen, L. Leiserowitz, and M. Lahav. 1998. Monitoring the nucleation of crystalline films of cholesterol on water and in the presence of phospholipid. *J. Phys. Chem. B*. 102:761–765.

Lipp, M. M., K. Y. C. Lee, D. Y. Takamoto, J. A. Zasadzinski, and A. J. Waring. 1998. Coexistence of buckled and flat monolayers. *Phys. Rev. Lett*. 81:1650–1653.

Lösche, M., E. Sackmann, and H. Möhwald. 1983. A fluorescence microscopic study concerning the phase diagram of phospholipids. *Ber. Bunsenges. Phys. Chem*. 87:848–852.

McIntosh, T. J., A. D. Magid, and S. A. Simon. 1990. Interactions between charged, uncharged, and zwitterionic bilayers containing phosphatidylglycerol. *Biophys. J*. 57:1187–1197.

McIntosh, T. J., and S. A. Simon. 1994. Hydration and steric pressures between phospholipid bilayers. *Annu. Rev. Biophys. Biomol. Struct*. 23: 27–51.

Meunier, J. 2000. Why a Brewster angle microscope? *Colloid. Surf. A. Physicochem. Eng. Asp*. 171:33–40.

Morris, S. J., D. Bradley, and R. Blumenthal. 1985. The use of cobalt ions as a collisional quencher to probe surface charge and stability of fluorescently labeled bilayer vesicles. *Biochim. Biophys. Acta*. 818:365–372.

Nag, K., J. Perez-Gil, M. L. Ruano, L. A. Worthman, J. Stewart, C. Casals, and K. M. Keough. 1998. Phase transitions in films of lung surfactant at the air-water interface. *Biophys. J*. 74:2983–2995.

Notter, R. H., S. A. Tabak, and R. D. Mavis. 1980. Surface properties of binary mixtures of some pulmonary surfactant components. *J. Lipid Res*. 21:10–22.

Notter, R. H., J. N. Finkelstein, and R. D. Taubold. 1983. Comparative adsorption of natural lung surfactant, extracted phospholipids, and artificial phospholipid mixtures to the air-water interface. *Chem. Phys. Lipids*. 33:67–80.

Orgeig, S., H. A. Barr, and T. E. Nicholas. 1995. Effect of hyperpnea on the cholesterol to disaturated phospholipid ratio in alveolar surfactant of rats. *Exp. Lung Res*. 21:157–174.

Peters, R., and K. Beck. 1983. Translational diffusion in phospholipid monolayers measured by fluorescence microphotolysis. *Proc. Natl. Acad. Sci. USA*. 80:7183–7187.

Piknova, B., W. R. Schief, V. Vogel, B. M. Discher, and S. B. Hall. 2001. Discrepancy between phase behavior of lung surfactant phospholipids and the classical model of surfactant function. *Biophys. J*. 81:2172–2180.

Piknova, B., V. Schram, and S. B. Hall. 2002. Pulmonary surfactant: phase behavior and function. *Curr. Opin. Struct. Biol*. 12:487–494.

Rand, R. P., and V. A. Parsegian. 1989. Hydration forces between phospholipid bilayers. *Biochim. Biophys. Acta*. 988:351–376.

Ries, H. E., Jr. 1979. Stable ridges in a collapsing monolayer. *Nature*. 281:287–289.

Ries, H. E., Jr., and H. Swift. 1987. Twisted double-layer ribbons and the mechanism for monolayer collapse. *Langmuir*. 3:853–855.

Saint-Jalmes, A., F. Graner, F. Gallet, and B. Houchmandzadeh. 1994. Buckling of a bidimensional solid. *Euro. Phys. Lett*. 28:565–571.

Saint-Jalmes, A., and F. Gallet. 1998. Buckling in a solid Langmuir monolayer: light scattering measurements and elastic model. *Eur. Phys. J. B*. 2:489–494.

Schief, W. R., L. Touryan, S. B. Hall, and V. Vogel. 2000a. Nanoscale topographic instabilities of a phospholipid monolayer. *J. Phys. Chem. B*. 104:7388–7393.

Schief, W. R., S. B. Hall, and V. V. Vogel. 2000b. Spatially patterned static roughness superimposed on thermal roughness in a condensed phospholipid monolayer. *Phys. Rev. E*. 62:6831–6837.

Schürch, S. 1982. Surface tension at low lung volumes: dependence on time and alveolar size. *Respir. Physiol*. 48:339–355.

Smith, R. D., and J. C. Berg. 1980. The collapse of surfactant monolayers at the air-water interface. *J. Colloid Interface Sci*. 74:273–286.

Takamoto, D. Y., M. M. Lipp, A. von Nahmen, K. Y. C. Lee, A. J. Waring, and J. A. Zasadzinski. 2001. Interaction of lung surfactant proteins with anionic phospholipids. *Biophys. J*. 81:153–169.

Vollhardt, D., and U. Retter. 1991. Nucleation in insoluble monolayers. 1. Nucleation and growth model for relaxation of metastable monolayers. *J. Phys. Chem*. 95:3723–3727.

Von Tscharner, V., and H. M. McConnell. 1981. An alternative view of phospholipid phase behavior at the air-water interface. Microscope and film balance studies. *Biophys. J*. 36:409–419.

Watkins, J. C. 1968. The surface properties of pure phospholipids in relation to those of lung extracts. *Biochim. Biophys. Acta*. 152:293–306.

Worthman, L. A., K. Nag, P. J. Davis, and K. M. Keough. 1997. Cholesterol in condensed and fluid phosphatidylcholine monolayers studied by epifluorescence microscopy. *Biophys. J*. 72:2569–2580.

Xue, J. Z., C. S. Jung, and M. W. Kim. 1992. Phase transitions of liquid-crystal films on an air-water interface. *Phys. Rev. Lett*. 69:474–477.

Ybert, C., W. X. Lu, G. Moller, and C. M. Knobler. 2002. Collapse of a monolayer by three mechanisms. *J. Phys. Chem. B*. 106:2004–2008.